ELSEVIER

Journal of Alloys and Compounds 216 (1994) 197–206

Journal of ALLOYS AND COMPOUNDS

Phase equilibria in the Ti–Te system

Holger Cordes, Rainer Schmid-Fetzer*

Technische Universität Clausthal, AG Elektronische Materialien, Robert-Koch-Straße 42, 38678 Clausthal-Zellerfeld, Germany

Received 1 April 1994

Abstract

The Ti–Te system was investigated using X-ray diffraction, optical microscopy, scanning electron microscopy, energy dispersive X-ray analysis and differential thermal analysis. Thermogravimetric vaporization measurements of $TiTe_2$ were performed to determine the phase boundaries between 67 and 50 at.% Te. Phase relations in the terminal regions Ti–Ti_5Te_4 and $TiTe_2$–Te could be clarified. The compound phases Ti_5Te_4, Ti_3Te_4, Ti_2Te_3, Ti_5Te_8 and $TiTe_2$ could be distinguished. Based on these data and a critical assessment of the literature a tentative phase diagram is constructed.

Keywords: Phase equilibria; Titanium; Tellurium

1. Introduction

The titanium–tellurium phase equilibria are of recent interest for the identification of reaction products between the contact metal Ti and the compound semiconductor CdTe. Although the Ti–Te system has been studied by various workers there are still many uncertainties about the number of equilibrium phases, their crystal structure and homogeneity ranges. An assessment of the system was made [1]; however, no phase diagram could be found in the literature. A vaporization study [2] indicated that the system is far more complex than assumed from earlier X-ray diffraction (XRD) studies. One experimental difficulty is the extreme reactivity in the atmosphere of compounds containing less than 50 at.% Te. In addition, there seems to be some confusion in the literature about phases and their crystal structures especially in the region between 40 and 60 at.% Te. Results from different annealing temperatures are probably not compatible. Some structures obviously belong to high temperature phases. In an early work [3] the region between 50 and 66.7 at.% Te was considered to be single phase (TiTe) with a continuous transition between the NiAs and CdI_2 structures. In a diffraction study [4] the region from 55.4 to 66.7 at.% Te was also considered as a single phase ($Ti_{2-x}Te_2$), but with a transition to monoclinic structure between 55.4 and 59.2 at.% Te, which was confirmed by later workers. The monoclinic part was designated Ti_3Te_4 [5]. In a later study this phase was supposed to have hexagonal structure in samples quenched from 800 °C and orthorhombic structure in samples quenched from 1000 °C [6].

The structure of Ti_5Te_4 phase was first found by Gronvold et al. [7] and confirmed by later workers. The existence of a Ti_2Te phase is questionable, since the suggested structure [8] is similar to Ti_5Te_4. It was suspected that this phase has a much smaller homogeneity range at lower temperatures and may disproportionate to Ti_5Te_4 and α-Ti [2].

In a vaporization study [2], some new phases, Ti_4Te_7, Ti_2Te_3 and $Ti_{10}Te_{19}$, were found but were not confirmed by XRD. However, the Ti_4Te_7 phase is very probably identical with the Ti_5Te_8 phase [9]. This structure can be observed also in related phase diagrams such as V–Te, V–S or Ti–Se, where it shows successive transformations to the M_3X_4 compound with the Cr_3S_4 structure and to the CdI_2 type when the temperature is raised [10].

The purpose of this study is (1) to clarify some of the uncertainties about the existence and structures of intermediate phases and (2) to construct the most likely phase diagram from our experiments and a critical assessment of literature data.

2. Experimental procedures and results

2.1. Preparation

Samples were prepared from the pure elements Ti (99.9 at.%) and Te (99.999 at.%) in evacuated and

*Corresponding author.

SSDI 0925-8388(94)01272-J

sealed silica ampoules. Ti powder (100 mesh) and Te pieces were mixed and pre-reacted in the closed ampoules with a gas flame and annealed at various temperatures. In samples with more than approximately 50 at.% Ti the composition might be shifted slightly to the Te side because of possible titanium–silica reactions. In these samples a thin layer with a TiSi compound was found which was estimated to change the overall composition of the sample by less than 3 at.%. After annealing at 500–1100 °C for 18–144 h the ampoules were quenched in water. One part of the sample was powdered for XRD analysis and one part was embedded in epoxy for scanning electron microscopy (SEM)–energy-dispersive X-ray analysis (EDXA). All Ti-rich samples with up to about 60 at.% Te were very porous (not completely melted) and these samples exhibited a phase segregation with the Ti phase on top.

2.2. Evaporation study

Thermogravimetric vaporization experiments were performed in a Netzsch simultaneous thermal analysis (differential thermal analysis (DTA)–thermal gravimetric analysis) apparatus with a Knudsen cell made from silica with a sealed-in capillary as an orifice. This vessel was filled with single-phase $TiTe_2$ powder, as identified by XRD and positioned on a thermogravimetric sample holder. The furnace was heated at 10 °C min^{-1} and the final temperature, 880–1180 °C, was kept constant for 10 h. The evaporation was studied under flowing argon at atmospheric pressure and the measured sample mass was corrected for buoyancy forces. During one of the experiments at 1180 °C the furnace was evacuated dynamically to approximately 10^{-2} mbar. The results are given in Figs. 1–4. From the measured mass loss vs. time curve the phase boundaries of the tellurides can be observed, since in mass spectrometric evaporation studies [2] no titanium or titanium tellurides were detected in the gas phase. The

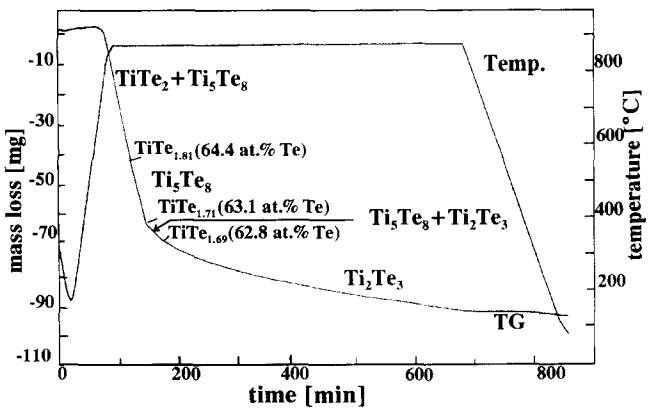

Fig. 1. Thermogravimetric vaporization curve starting with $TiTe_2$ at 880 °C under flowing argon at 1 bar.

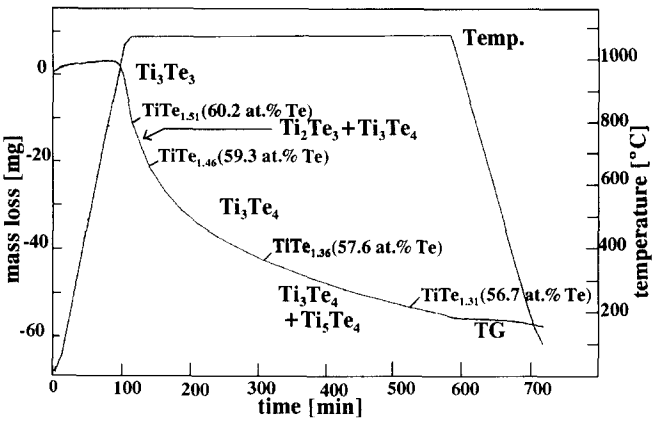

Fig. 2. Thermogravimetric vaporization curve starting with 61 at.% Te (residual mass of Fig. 1) at 1080 °C under flowing Ar at 1 bar.

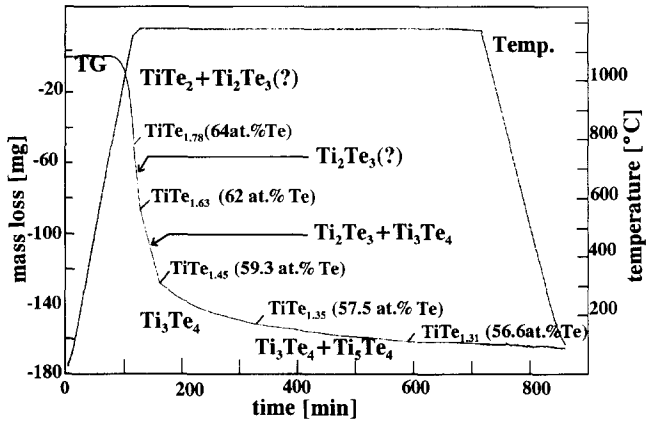

Fig. 3. Thermogravimetric vaporization curve starting with $TiTe_2$ at 1180 °C under flowing Ar at 1 bar. The phase field of Ti_5Te_8 could not be observed and may be obscured in Ti_2Te_3.

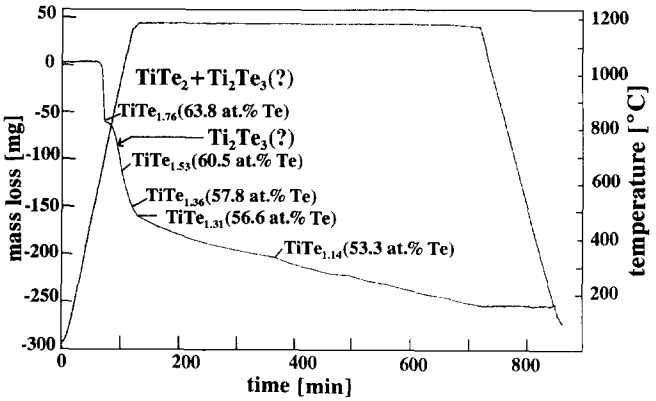

Fig. 4. Thermogravimetric vaporization curve starting with $TiTe_2$ at 1180 °C under dynamic vacuum (10^{-2} mbar). See also the note on Fig. 3.

bends of the mass loss curves are labelled in Figs. 1–4 with the corresponding stoichiometries $TiTe_x$, calculated from the tellurium loss. If there are two condensed phases in equilibrium with the gas phase, the rate of mass loss is constant, since the Te vapor pressure is constant. Hence the observed curve should be linear

in two-phase regions and curved in single-phase regions. For a stoichiometric phase just a sharp bend between two linear regimes would be observed. The composition of the sample at sharp bends in the curve determines the phase boundaries. The one- and two-phase fields assigned in Figs. 1–4 will be discussed later.

2.3. X-ray diffraction

After powdering of the annealed samples, detailed in Section 2.1, the XRD analysis had to be performed immediately because of the high reactivity of some tellurides in atmospheric conditions. A Siemens D5000 diffractometer with Cu Kα radiation and Ni filter was used. The indexing of the spectra and lattice parameter calculations were performed with the support of industrial computer programs (WINDEX and WINMETRIC). Owing to the experimental difficulty of obtaining single-phase samples there are many discrepancies in the literature and the corresponding Joint Committee on Powder Diffraction Standards data in some cases might be questionable; this will be discussed in detail in Section 3. It was attempted in this study to produce single-phase samples in the following way. If the sintered pellets appeared to be two-phase by optical inspection after breaking the silica tube, it was attempted to separate the phases roughly with tweezers and then the phases were analyzed independently using XRD. Care was taken to remove completely all the occasional thin silicide layers. Still most samples were not completely single phase which often resulted in some minor lines that could not be indexed.

All sample compositions, annealing conditions and identified phases are compiled in Table 1. X-ray spectra demonstrating the phase sequence from $TiTe_2$ to Ti_2Te_3 are given in Fig. 5. The spectra of Ti_5Te_4, taken from three samples in the (Ti) + Ti_5Te_4 field after mechanical separation of (Ti), are given in Fig. 6.

2.4. Differential thermal analysis

All samples for DTA were sealed in evacuated thin-walled special silica tubes. From preliminary DTA measurements on samples, which had been previously stored in air, a large low temperature peak due to oxidation occurred. Therefore all samples were directly prepared from the elements in DTA silica tubes, pre-reacted with the gas flame, and quenched and annealed at 600 °C for 24 h before the measurement. After this procedure, no oxidation peak occurred. Another potential error source is the formation of silicide in the samples. On a sample with pure Ti powder, which was not pre-annealed, an exothermic peak at approximately 760 °C occurred, presumably because of the reaction with the silica. On pre-annealed Ti-rich alloy samples this peak was not observed.

The results of the experiments are plotted in the proposed phase diagram in Figs. 7 and 8. All samples were measured at heating and cooling rates of 10 °C min^{-1}. There was no significant change in peak temperatures in measurements at a slower heating rate. The given values are the extrapolated peak onset temperatures, since the actual beginning of a reaction was often difficult to detect. Some thermal signals were rather small and in some cases broad peaks were observed owing to sluggish reactions. These questionable temperature values are denoted by open triangles in Figs. 7 and 8. Owing to the limited durability of the thin-walled silica tubes the maximum temperature was approximately 1200 °C and the liquidus line could be measured only in the Te-rich corner up to the $TiTe_2$ phase. Two Ti-rich samples were heated to 1350 °C in thick-walled silica tubes to measure the eutectic temperature, 1280 °C. The silica softened but still encapsulated the sample because the vapor pressure was low enough in this region of the system.

2.5. Metallography and electron probe microanalysis

After the DTA run the samples were embedded in epoxy and prepared metallographically; the cross-section was analyzed both with optical microscopy and SEM–EDXA. The standardless analysis is not very accurate because of a peak overlap between K_α(Ti) and L_γ(Te). A deconvolution of peak overlaps could not be done. In particular for Te-rich phases ($TiTe_2$) the EDXA-measured Ti content was higher than the as-weighed sample composition by some 8 at.% Ti. It was not possible to detect oxygen contaminations, since a standard detector with beryllium window was used. The EDXA was therefore not suitable for the determination of the exact homogeneity ranges. However, the EDXA data are reproducible enough to identify the phases in the cross-sectioned DTA samples. The relative error is smaller in phases with a low Te content.

By comparison of the compositional data with the XRD results all phases present in the sample were identified. The compositions which were measured in the solidified DTA samples have been tabulated elsewhere [11]. The micrograph of a cross-section from a solidified Ti–33at.%Te sample given in Fig. 9 demonstrates the existence of the eutectic reaction $L \rightleftharpoons \beta\text{-}Ti + Ti_5Te_4$. In EDXA measurements on the solidified DTA samples, values in the range 1–3 at.% Te were found in the Ti phase. In the backscattered electron image of the titanium phase, two different regions with approximately 1 or 3 at.% could be distinguished. With higher resolution a very fine-structured two-phase region was found in the region with 3 at.% Te which cannot be seen in Fig. 9 because of the contrast setting. Therefore a eutectoid reaction $\beta\text{-}Ti \rightleftharpoons \alpha\text{-}Ti + Ti_5Te_4$ at

Table 1
Composition, annealing conditions and identified phases of the X-ray diffraction study

Composition (at.%)	Annealing conditions		Lattice type indexed[a]	Lattice parameters				Phases	Comment
	Temperature (°)	Time (h)		a (nm)	b (nm)	c (nm)	β (°)		
$Ti_{33.3}Te_{66.7}$	800	50	h	0.3770	–	0.6492	–	$TiTe_2$	Single phase
$Ti_{36.3}Te_{63.7}$	800	20	h	0.3824	–	0.6423	–	Ti_5Te_8	Single phase
$Ti_{37.7}Te_{62.3}$	1000	42	h	0.3815	–	0.6434	–	Ti_5Te_8	Single phase, large crystallites
$Ti_{38.5}Te_{61.5}$	800	20	h	0.3874	–	1.2723	–	Ti_2Te_3	Single phase, superstructure
$Ti_{40.6}Te_{59.4}$	1000	42	h	0.3887	–	1.2699	–	Ti_2Te_3	Single phase, superstructure
$Ti_{42.5}Te_{57.5}$	1100	19	h	0.389	–	1.269	–	β-Ti_3Te_4	Bottom part was brown colored (Ti_3Te_4)
			t	1.0162	–	0.3771	–	Ti_5Te_4	Upper part of the sample was dark gray (Ti_5Te_4)
$Ti_{44.5}Te_{55.5}$	1000	20	h	0.3887	–	1.269	–	β-Ti_3Te_4	Bottom part was brown colored (Ti_3Te_4)
			t	1.0162	–	0.3771	–	Ti_5Te_4	Upper part of the sample was dark gray (Ti_5Te_4)
$Ti_{44.5}Te_{55}$	500	144	h	0.3871	–	1.2717	–	β-Ti_3Te_4	Bottom part only
$Ti_{50}Te_{50}$	1000 (slowly cooled)	20	m	0.6913	0.3846	1.2673	90.385	α-Ti_3Te_4	Bottom part only
$Ti_{51.8}Te_{48.2}$	400[b]	20[b]	t m	1.0162 0.69232	– 0.38406	0.3771 1.26578	– 90.468	Ti_5Te_4 Ti_3Te_4	
$Ti_{56}Te_{44}$	1000	22	t	1.01622	–	0.37706	–	Ti_5Te_4,	Trace amount of Ti_3Te_4
$Ti_{60.2}Te_{39.8}$	1000	18	t	1.01619	–	0.37673	–	Ti_5Te_4 (Ti)	
$Ti_{67}Te_{33}$	1100	20	t	1.0162	–	0.3771	–	Ti_5Te_4 (Ti)	
$Ti_{73}Te_{27}$	400[b]	72[b]	t	1.0162	–	0.3771	–	Ti_5Te_4 (Ti)	
$Ti_{81}Te_{19}$	1000	20	t	1.0162	–	0.3771	–	Ti_5Te_4 (Ti)	
$Ti_{83}Te_{17}$	400[b]	70[b]	t	1.0162	–	0.3771 (Ti)	–	Ti_5Te_4	
$Ti_{90}Te_{10}$	1000	20	t	1.01633	–	0.3769		Ti_5Te_4 (Ti)	

[a]h, hexagonal; t, tetragonal; m, monoclinic.
[b]Sample was pre-annealed at 1100 °C.

approximately 3 at.% Te (β-Ti) and 1 at.% Te (α-Ti) can be concluded.

3. Discussion

The proposed phase equilibria are given in Figs. 7 and 8, and the data on the accepted solid phases in Table 2. Additional solid phases, reported in the literature but not accepted as stable phases, are compiled in Table 3. The phase relations in the two terminal regions from Ti to Ti_5Te_4 and from Te to $TiTe_2$ are at least qualitatively clear; the liquidus lines and some solubility limits had to be estimated. One major finding is the existence of the eutectic reaction $L \rightleftharpoons \beta\text{-Ti} + Ti_5Te_4$ at 1280 °C with a liquid content of around 20 at.% Te based on the DTA and metallographic data. The maximum solubility of about 5 at.% Te in β-Ti was

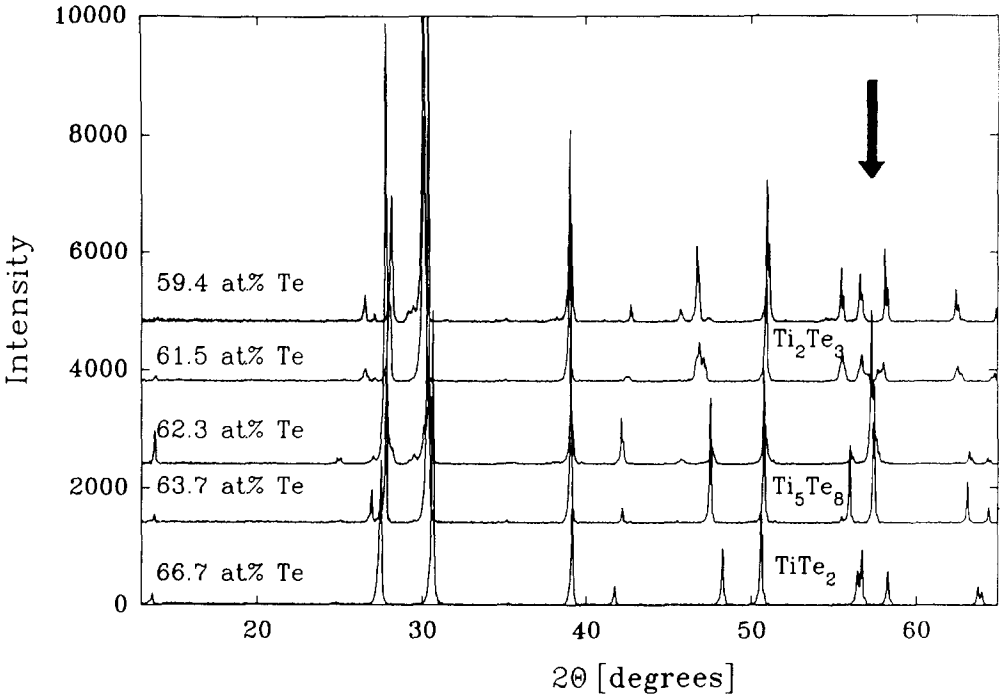

Fig. 5. XRD spectra of quenched samples in the Te content range 59.4–66.7 at.%, annealed at 800–1000 °C. The arrow denotes a region where a transformation from the $TiTe_2$ phase to the Ti_5Te_8 and Ti_2Te_3 phases is observed.

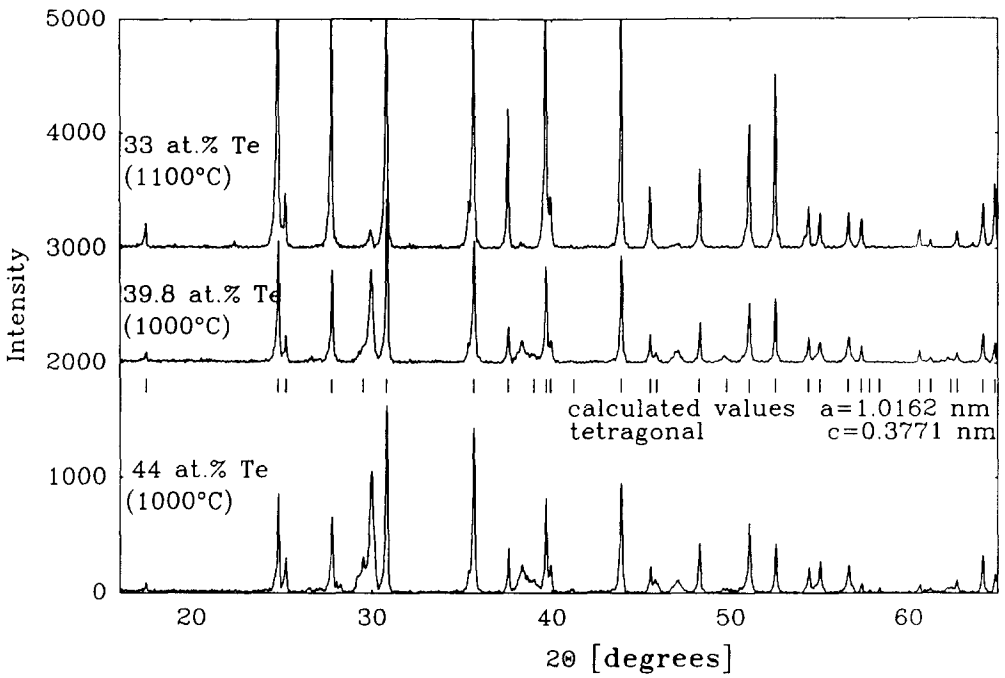

Fig. 6. XRD spectra of the Ti_5Te_4 phase in samples of different compositions taken at room temperature. The (Ti) phase was separated before the analysis of sample. No other phase additional to Ti_3Te_4 could be detected, except for a trace amount of Ti_3Te_4 in the sample with 44 at.% Te.

estimated to be somewhat higher than the value of 3 at.% Te at the eutectoid at 860 °C. The existence of this eutectoid, $\beta\text{-Ti} \rightleftharpoons \alpha\text{-Ti} + Ti_5Te_4$, is clearly seen from microstructural SEM–EDXA and also from DTA. The DTA data scatter at around 840 °C upon heating and 875 °C upon cooling, which is lower than the α–β transition of pure Ti, found at 858 °C upon heating and 885 °C upon cooling. The values for Ti indicate some oxygen contamination.

Both the eutectic and the eutectoid are in contradiction to the proposal of Suzuki and Wahlbeck [2] who suggested a huge Te solubility in α-Ti (25 at.%

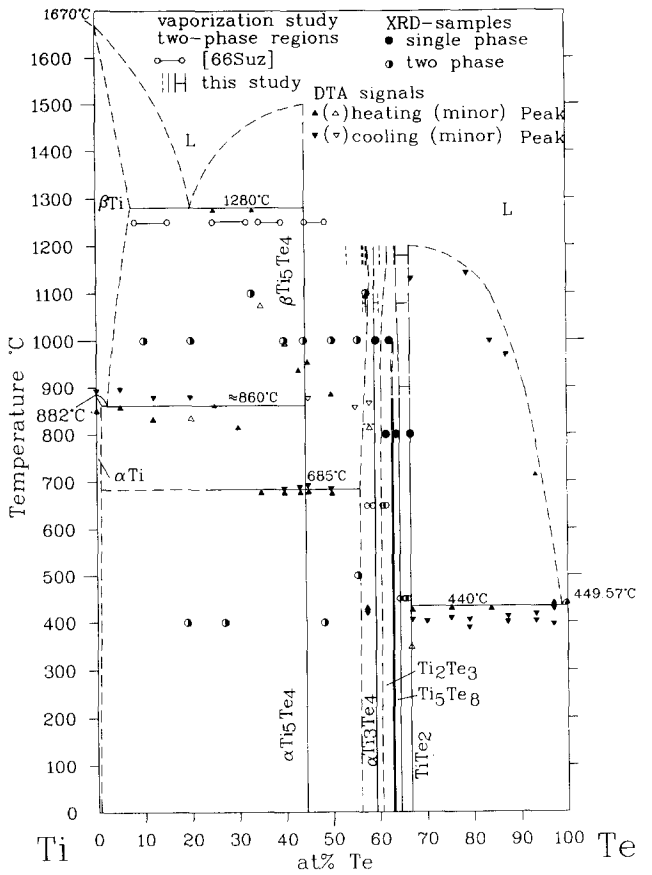

Fig. 7. Tentative Ti–Te phase diagram with present XRD and DTA data and phase boundaries, detected by isothermal vaporization, including also the data of Suzuki and Wahlbeck [2].

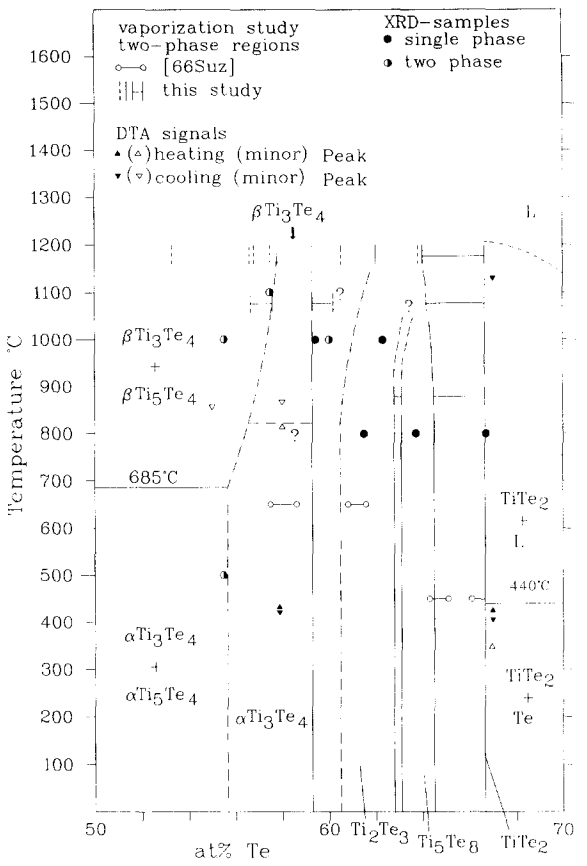

Fig. 8. Expanded region (50–70 at.% Te) of the Ti–Te phase diagram.

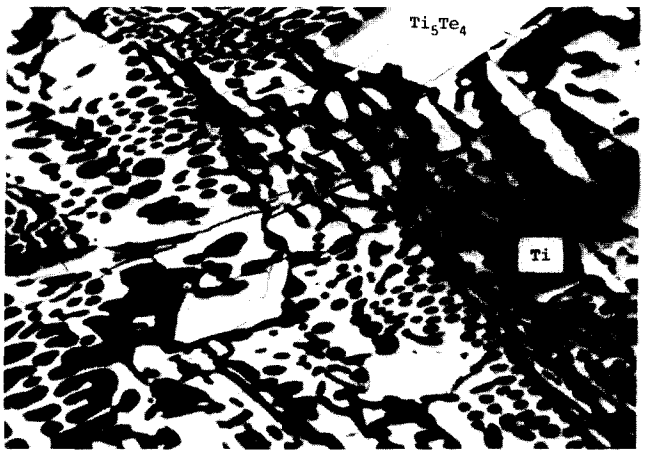

Fig. 9. Micrograph of a DTA sample with 33 at.% Te, solidified from 1330 °C, demonstrating the eutectic reaction $L \rightleftharpoons \beta\text{-Ti} + \beta\text{-Ti}_5Te_4$ with Ti_5Te_4 primary crystals (backscattered-electron image). The dark Ti regions consist of (Ti) and a eutectoid structure, which is not visible with this contrast setting.

Te) and an increase in the α–β transition temperature with (β-Ti + α-Ti) in equilibrium at 1250 °C. This proposal is rejected in view of the present data since it was based on the breaks in the vaporization curves at 1250 °C, which are difficult to detect [2].

The solubility of Te in α-Ti is around 1 at.% Te at 860 °C, estimated from the present EDXA data. This is considerably higher than the solubility of 0.18 at.% Te suggested earlier [19]. No other compound could be detected between Ti and the line compound Ti_5Te_4.

On the Te-rich side of the phase diagram in Fig. 7 a eutectic $L \rightleftharpoons Te + TiTe_2$ could be clearly detected from SEM–EDXA and by DTA. Only the DTA data on heating were evaluated to find 440 °C as the eutectic temperature, since the cooling data are prone to supercooling. No additional phase could be detected between the line compound $TiTe_2$ and Te; all samples were two phase ($TiTe_2$ + Te). The solubility of Ti in Te was below the EDXA detection limit.

The region between the most clearly identified line compounds $TiTe_2$ and Ti_5Te_4 is more ambiguous and no liquidus data are presented. The phases within this region, Ti_5Te_8, Ti_2Te_3 and Ti_3Te_4, all exhibit a homogeneity range. The more certain phase boundaries are given by full lines in Fig. 8. They are based primarily on the clearly detected two-phase regions from the present vaporization study, plotted as full symbols in Fig. 8. Due consideration was also given to all the other data. The two-phase data from the vaporization study of Suzuki and Wahlbeck [2] are plotted in Fig. 8 for comparison. These data are not in agreement with the accepted phase boundaries; however, the breaks

Table 2
Accepted solid phases, crystal structures and temperature stabilities in the Ti–Te system

Phase	Te content (at.%)	Pearson symbol	Space group	Prototype	Lattice parameters				Temperature stability (°C)	Reference
					a (nm)	*b* (nm)	*c* (nm)	*β* (°)		
(*β*-Ti)	0–≈5	cI2	$Im\bar{3}m$	W	0.33065	–	–	–	1670–860	[12], this study
(*α*-Ti)	0–0.18	hP2	$P6_3/mmc$	Mg	0.29506	–	0.46835	–	<882	[12]
	0–1									This study
(Te)	100	hP3	$P3_121$	*γ*-Se	0.44566	–	0.59264	–	<449.57	[12]
β-Ti_5Te_4	44.4								Minimum 1350–685	This study[a]
α-Ti_5Te_4	44.4	tI18	*I*4/*m*	Ti_5Te_4	1.0164	–	0.3772	–	600[b]	[7,4]
	44.4	t..			1.0162	–	0.3771	–	<685	This study
β-Ti_3Te_4		h..			0.6713	0.3876 ?	0.6361	–	800[b]	[6]
		o..			0.6804	0.3860	0.6341×2	–	1000[b]	[6]
	57.5–59.3	h..			0.3887	–	1.269	–	1100[b]	This study
α-Ti_3Te_4	55–57.6	mC14	*C*2/*m*	Cr_3Se_4	0.6982	0.385	1.266	90.47		[5]
	55.4–59.2	m..			0.6954–0.6840	0.3836–0.3850	1.2716–1.2658	90.63–90.42	600[b]	[4]
		m..			0.6902	0.3835	0.6331×2	90.55	600[b]	[6]
		m..		Cr_3S_4	0.6920	0.3840	1.266	90.50	300[b]	[13]
	55.4–59.2	m..			0.6923	0.3841	1.2658	90.47	400[b]	This study
Ti_2Te_3	60.0	h..			0.3878		0.6350	–	800[b]	[14]
	60.5–62.8	h..			0.3874	–	1.2723	–	800[b]	This study
Ti_5Te_8	60–62.96	h..		Ti_5Se_8	0.7686	–	1.2786	–	1050[b]	[9]
	63.1–64.4	h..			0.3824	–	0.6423	–	800[b]	This study
$TiTe_2$	66.67	hP3	$P\bar{3}m1$	CdI_2	0.3777	–	0.6495	–		[15]
	≈60–66.7	h..			0.3884–0.3766	–	0.6348–0.6491	–		[4]
		h..			0.3777	–	0.6498	–		[19]
	66.7	h..			0.3770	–	0.6492	–	⩽1200±20	This study

[a]Phase transition between *α*-Ti_5Te_4 and *β*-Ti_5Te_4 at 685 °C observed by pronounced DTA signals only.
[b]Annealing temperature.

Table 3
Additional solid phases from the literature, not accepted as stable phases

Phase	Te content (at.%)	Pearson symbol	Space group	Prototype	Lattice parameters				Temperature stability (°C)	Reference
					a (nm)	*b* (nm)	*c* (nm)	*β* (°)		
Ti_3Te_2	30	t..			1.43	–	0.358	–		[17]
Ti_2Te	25–33.3	t..			1.43	–	0.36	–	800[a]	[8]
Ti_2Te		t..								[2]
TiTe	44–50	h..			0.770	–	1.262	–		[17]
	50	h..			0.383	–	0.639	–		[8]
	50	hP4	$P6_3/mmc$		0.3834	–	0.635	–		[14]
	50	hP4	$P6_3/mmc$		0.3834	–	0.6390	–		[18]
Ti_4Te_7		–	–		–	–	–	–		[2]
$Ti_{10}Te_{19}$		–	–		–	–	–	–		[2]

[a]Annealing temperature.

in the published original vaporization curve [2] are much less pronounced than the clear breaks in Figs. 1 and 3.

The data collected on all compound phases in the Ti–Te system are discussed below in comparison with literature data.

3.1. $TiTe_2$

The sample with 66.7 at.% Te is clearly a hexagonal single phase; the lattice parameters (Table 1) are in agreement with the literature data (Table 2). The composition range, reported by Raaum et al. [4] only, could not be found; $TiTe_2$ is accepted as a line compound. Its melting point (1200 ± 20 °C) is estimated to be above 1180 °C from the vaporization experiments and the DTA data, which are, however, prone to supercooling. It is unclear whether $TiTe_2$ is actually a congruently melting compound as indicated by the broken liquidus line in Fig. 7. At atmospheric pressure the compound decomposes at approximately 700 °C (Fig. 1).

The existence and structure of $TiTe_2$ has also been reported in very early papers [3,20]. There was no evidence in the metallographic sections, the evaporation study or the XRD measurements for a phase "$TiTe_{1.9}$" which was suggested by Suzuki and Wahlbeck [2]. It is believed that this phase boundary was observed because the initial composition in the vaporization experiment [2] was not single phase but had a slight Te surplus.

3.2. Ti_5Te_8

This phase was originally designated Ti_5Te_8 by Brunie and Chevreton [9] who found a phase similar to $TiTe_2$ but with doubled hexagonal unit-cell parameters in samples between 60 and 62.96 at.% Te, slowly cooled from 1050 °C. This composition range is not compatible with our evaporation study (63.1–64.4 at.% Te at 880 °C). The X-ray spectra of our Ti_5Te_8 single-phase samples at 63.7 and 62.3 at.% Te could be indexed with a hexagonal unit cell and lattice parameters similar to $TiTe_2$ (see Table 1).

It is important to note that the XRD spectra in the Te content range 66.7–59.4 at.% look very similar (Fig. 5). In other words the phases $TiTe_2$, Ti_5Te_8 and also Ti_2Te_3 are closely related.

This kind of phase transition may be compared with the order–disorder transformations in the V–S and V–Se systems, where a second-order transformation from V_5S_8 to V_3S_4 type and finally to CdI_2 type occurs upon heating [10].

In the present Ti–Te case the transition is clearly of first order, at least at 880 °C, since Ti_5Te_8 is definitely bound by two-phase regions from the vaporization data. At higher temperatures the Ti_5Te_8 phase field may be cut off, as indicated in Fig. 8, since at 1180 °C essentially only one phase region (62–64 at.% Te) is present.

The " Ti_4Te_7" phase of Suzuki and Wahlbeck [2] , found in a stoichiometry range from 61.8 to 64.3 at.% Te (450 °C), is likely to be identical with the Ti_5Te_8 phase.

3.3. Ti_2Te_3

The phase Ti_2Te_3 is closely related to Ti_5Te_8; however, they can be clearly distinguished by the occurrence of additional peaks in the XRD spectra at around $2\Theta \approx 57°$ (Fig. 5). The sample with 61.5 at.% Te, annealed at 800 °C, was also found to be single phase in the metallographic analysis. An indexing with an approximately doubled *c* axis gave a much better fit for Ti_2Te_3 than for Ti_5Te_8. The Te-rich phase boundary at 62.8 at.% Te is very clear from the vaporization data at 880 °C. The Ti-rich boundary is given with an estimated

60.5 at.% Te at lower temperatures and a clear value of 62 at.% Te from the pronounced vaporization data at 1180 °C. The evaporation data in [2] indicate a phase labelled as Ti_2Te_3 in the range 59.0–60.9 at.% Te at 600–700 °C, which is lower than the present data.

3.4. Ti_3Te_4

Two modifications of Ti_3Te_4 exist. The monoclinic room-temperature phase of Ti_3Te_4 was found in two-phase samples with 48.2 and 50 at.% Te, slowly cooled or annealed at 400 °C. The lattice parameters are in agreement with the literature data (Table 2). The phase boundaries are taken from the extensive study of Raaum et al. [4], who considered α-Ti_3Te_4 as part of the "$Ti_{2-x}Te_2$" phase and noted the resemblance to a monoclinic deformed NiAs-like structure type. The structure is probably more accurately described as Cr_3S_4 type [5], also found in an investigation of the systems $(Cr_yTi_{1-y})_3X_4$ for X≡Se, Te [14]. These systems are homogeneous for $y=0$ to 1 with the monoclinic Cr_3S_4-type structure.

It is interesting to note that the Cr_3S_4-type structure can be derived from the CdI_2 type as demonstrated by Ueda et al. [14], and in fact the Ti_3Se_4 phase inhibited an order–disorder transformation upon heating at 900 °C to the CdI_2-type structure. In other words this phase and likewise α-Ti_3Te_4 are also closely related to $TiTe_2$ with CdI_2 structure. This relationship was also seen in the similarity of the present X-ray spectra; however, the resemblance within the phase bundle $TiTe_2$–Ti_5Te_8–Ti_2Te_3 (Fig. 5) is closer than with α-Ti_3Te_4. This agrees also with the findings of Raaum et al. [4].

Samples in the α-Ti_3Te_4 composition range quenched from higher temperatures could be indexed somewhat better in the hexagonal than in the monoclinic lattice, indicating the existence of a closely related high temperature form, β-Ti_3Te_4. Small DTA signals occurred in this composition range at around 850 °C. It is assumed that they indicate the α-Ti_3Te_4/β-Ti_3Te_4 transition which may be of second order, in view of the similarity to Ti_3Se_4 [14]. Two of our samples do not agree with an 850 °C transition temperature: one is the 55 at.% Te sample annealed at 500 °C (Table 1), and the other is the residual amount with about 56.5 at.% Te from the vaporization experiment in Fig. 2, slowly cooled from 1080 °C within 100 min. Both samples are indexed as hexagonal with lattice parameters of β-Ti_3Te_4.

The composition range of β-Ti_3Te_4 at high temperatures is narrower than for α-Ti_3Te_4. Rather clear vaporization data indicate a range 57.6–59.3 at.% Te at 1080 °C and 57.5–59.3 at.% Te at 1180 °C for β-Ti_3Te_4. The boundary at 59.3 at.% Te is most pronounced and also agrees with the solubility limit for α-Ti_3Te_4 at 600 °C [4].

In addition to the monoclinic (at 600 °C) and hexagonal form (at 800 °C) an additional orthorhombic form (at 1000 °C) of Ti_3Te_4 was proposed by Arnaud and Chevreton [6]. However, there is at least one typing error in their tabulated lattice parameters, since $a \neq b$ for hexagonal β-Ti_3Te_4, as reproduced in Table 2 and labelled with a question mark. The X-ray spectra of α-Ti_3Te_4 observed in the present study are far from an orthorhombic lattice and such a form of Ti_3Te_4 is not accepted.

3.5. Ti_5Te_4

The Ti_5Te_4 phase was clearly identified as a stoichiometric line compound in agreement with the conclusions of Gronvold et al. [7] and Raaum et al. [4], who based the stoichiometry on a sharp bend in the density vs. composition curve and the determination of the Ti_5Te_4 structure [7].

The lattice parameters are in perfect agreement with our data from the sample with 44 at.% Te (Table 2); however, in contrast with the work of Raaum et al. [4], who found no extra peaks, there were some extra peaks in our spectrum, which belong obviously to the Ti_3Te_4 phase. With increasing Ti content these lines vanished (see Fig. 6). Two explanations are suggested for this finding.

Firstly, there is always a slight Ti loss due to reaction with the silica which shifts the overall composition, Secondly, small amounts of metallic titanium were found in the samples, in addition to the Ti_3Te_4 traces, indicating that the reaction of the elemental starting components may not be completed.

The former suggests more Ti-rich phases Ti_2Te [8] or Ti_3Te_2 [17] which are presumably identical with Ti_5Te_4 [4], since the observed structures are very similar. In both studies needle-like single crystals were observed; these were also found in our solidified DTA samples, e.g. at 33.3 at.% Te. The fact that Ti_5Te_4 is the Ti-richest compound in this system is confirmed by the present XRD study on samples with Ti contents down to 10 at.%, annealed at 1000 °C and quenched or slowly cooled (see Table 1). In all cases the tetragonal Ti_5Te_4 spectrum was observed with the same lattice parameters. The additional (Ti) phase could not be pulverized in the mortar.

4. Conclusion

Based on a variety of experimental methods the phase equilibria in the terminal regions Ti–Ti_5Te_4 and $TiTe_2$–Te are revealed; the intermediate range is more ambiguous. A tentative phase diagram is presented for the first time in Figs. 7 and 8. Major new findings are as follows: the eutectic $L \rightleftharpoons \beta\text{-Ti} + \beta\text{-}Ti_5Te_4$ at 1280 °C,

the eutectoid β-Ti $\rightleftharpoons$ α-Ti + β-Ti_5Te_4 at 860 °C, the eutectic L $\rightleftharpoons$ Te + $TiTe_2$ at 440 °C, the partial liquidus line of $TiTe_2$ and a transition α-Ti_5Te_4–β-Ti_5Te_4 at 685 °C. Data on the stoichiometric phases Ti_5Te_4 and $TiTe_2$ and on the homogeneity ranges of the intermediate phases Ti_3Te_4, Ti_2Te_3 and Ti_5Te_8 are more or less compatible with the majority of the work in the literature. The conflict with the phase boundaries suggested in the vaporization study of [2] and reproduced in [1] has been discussed.

Future work is needed to reveal the melting equilibria and some ambiguities in the range between Ti_5Te_4 and $TiTe_2$. A high temperature X-ray investigation of β-Ti_5Te_4 is also suggested.

Acknowledgement

The authors wish to acknowledge financial support of this work from the Deutsche Forschungsgemeinschaft in the focal program "II–VI semiconductor structures".

References

[1] J.L. Murray, The Te–Ti system, *Phase Diagrams of Binary Titanium Alloys,* American Society for Metals, Metals Park, OH, 1987, pp. 309–310.

[2] A. Suzuki and P.G. Wahlbeck, Vaporization study of the titanium–tellurium system, *J. Phys. Chem., 6* (1966) 1914–1923.

[3] P. Ehrlich, Über Titanselenide und -telluride, *Z. Anorg. Chem., 260* (1949) 1–18.

[4] F. Raaum, F. Gronvold, A. Kjekshus and H. Haraldson, Über das System Titan–Tellur, *Z. Anorg. Chem., 317* (1962) 91–104.

[5] M. Chevreton and F. Bertaut, Étude de séléniures de titane et de vanadium et de tellurure de titane, *C.R. Acad. Sci., 255* (1962) 1275–1277.

[6] Y. Arnaud and M. Chevreton, Étude structurale de séléniures, tellurures et selenio-tellurures de titane $Ti_3Se_{4-x}Te_x$ ($0<x<4$), *J. Solid State Chem., 9* (1974) 54–62.

[7] F. Gronvold, A. Kjekshus and F. Raaum, The crystal structures of Ti_5Te_4, *Acta Crystallogr., 14* (1961) 930–934.

[8] H. Hahn and P. Ness, Über Subchalkogenidphasen des Titans, *Z. Anorg. Chem., 302* (1959) 17–36.

[9] S. Brunie and M. Chevreton, Étude structurale du composé Ti_5Te_8, *Mater Res. Bull., 3* (1968) 309–314.

[10] Y. Oka, K. Kosuge and S. Kachi, Order–disorder transition of the metal vacancies in the vanadium–sulfur system. I. An experimental study, *J. Solid State Chem., 23* (1978) 11–18.

[11] H. Cordes, *Dr.-Ing. Thesis,* Technische Universität Clausthal, 1994.

[12] T.B. Massalski (ed.), *Binary Alloy Phase Diagrams,* American Society for Metals, Metals Park, OH, 2nd edn., 1990.

[13] Y. Ueda, K. Kosuge, M. Urabayashi, A. Hayashi and S. Kachi, Phase diagram and metal distribution of the $(Cr_xTi_{1-x})Se_4$ system ($0<x<1$) with the Cr_4S_4-type structure, *J. Solid State Chem., 56* (1985) 263–267.

[14] F.K. McTaggart and A.D. Wadsley, The sulphides, selenides and tellurides of titanium, zirkonium, hafnium and thorium, I. Preparation and characterization, *Aust. J. Chem., 11* (1958) 445–457.

[15] C. Riekel, M. Thomas and R. Schöllhorn, Structure refinement on stoichiometric $TiTe_2$ by neutron diffraction, *Phys. Status Solidi, 50* (1978) K231–K234.

[16] Y. Arnaud and M. Chevreton, Étude comparative des composés TiX_2 (X = S, Se, Te). Structures de $TiTe_2$ et TiSeTe, *J. Solid State Chem., 39* (1981) 230–239.

[17] H. Hahn and P. Ness, Zur Frage der Existenz von Subchalkogenidphasen des Titans, *Naturwissenschaften, 44* (1957) 581.

[18] X. Oudet, Structures cristallines et liaisons, *Ann. Chim., 8* (1983) 483–507.

[19] R.M. Goldhoff, H.L. Shaw, C.M. Craighead and R.I. Jaffee, The influence of insoluble phases on the machinability of titanium, *Trans. Am. Soc. Met., 45* (1953) 941–971.

[20] I. Oftedal, X-ray investigation of SnS_2, TiS_2, $TiSe_2$, $TiTe_2$, *Z. Phys. Chem., 134* (1928) 301–310.